COMPUTATIONAL CONTINUUM MECHANICS

ВЫЧИСЛИТЕЛЬНАЯ МЕХАНИКА СЛОШНЫХ СРЕД

Computational Continuum Mechanics. 2021. Vol. 14. No. 2. pp. 203-209 DOI: 10.7242/1999-6691/2021.14.2.17

ROLE OF CRISTON SHEAR SOURCES IN THE FORMATION OF CHERNOV–LUDERS BANDS

M.P. Kashchenko[1,2], A.G. Semenovykh[2], A.V. Nefedov [2], N.M. Kashchenko[1] and V.G. Chashchina[1,2]

[1]*Ural Federal University, Yekaterinburg, Russian Federation*
[2]*Ural State Forestry University, Yekaterinburg, Russian Federation*

Shear bands often appear during plastic deformation. The Chernov–Luders band is an example of a complex multiscale heterogeneous structure containing shear bands. The article is devoted to the analysis of a part of the experimental data on the formation (under tension) of the Chernov–Luders band in textured polycrystalline steel samples with fine grain, pre-deformed by rolling. The main focus is on the criston mechanism of formation of the observed texture components. The essence of the criston approach, associated with the contact interaction of dislocations at the intersection of slip planes, is briefly outlined. The information on the observed types of texture is given and a sufficiently detailed analysis of the reconstruction of the mechanism of the appearance of several texture components is carried out taking into account the interaction of the main dislocation slip systems for a body-centered cubic (bcc) lattice. It is shown that some of the real shear directions correspond to the interaction of more than two dislocation slip systems, that is, in fact, there are criston-cristons combinations. A summary table of the results of the analysis of the "composition" of cristons for all texture components is presented, reflecting the fractional contribution of dislocations belonging to interacting slip systems. The analysis has shown that practically all systems of standard slip along the planes of the {110}, {112}, {123} families play an active role in the formation of cristons and, accordingly, the observed texture. Brief summary comments are provided. In particular, it was noted that, with a sequential criston approach, the issue of non-Schmidian slip variants can be eliminated. The role of texturing is also noted for the ordering of the intergranular medium and the appearance of macroconcentrators in groups of contacting grains, which, as experience shows, are important in the formation of the Chernov–Luders band, is emphasized.

Key words: dislocations, cristons, shear bands, Chernoff–Luders band, texture components

1. Introduction

The formation of the Chernov-Luders bands (CLB) occurs during plastic deformation and is a complex hierarchical process that proceeds in a consistent manner at several scale levels. This feature has been repeatedly highlighted in the literature (see, for example, [1–3]). In particular, the formation of CLB in alloys with a body-centered cubic (bcc) lattice in the macroscopic description of the curve $(\sigma - \varepsilon)$ (stress – strain) shows an abrupt decrease followed by a plateau-like area ("yield tooth"). Moreover, the plateau itself (fluidity area) may consist of smaller jumps. Most often, CLBs are observed in tensile experiments on polycrystalline samples. The angles between the normals to the CLB macro boundaries and the direction of tensile are usually within a segment (45–60 °). CLB is structurally heterogeneous; its internal striped structure was found. Inner shear bands have borders that are not necessarily parallel to each other. When CLB occurs, the main deformation localized precisely in the shear bands. The lattice inside the CLB is clearly turning. Hence, disclination models can be used to describe the CLB formation process. From the kinetic point of view, the slow (with a speed of $\sim 10^{-5}$ m / s) broadening of the CLB finds a rather clear interpretation in the propagation of fronts [3, 4]. Apparently, the lattice curvature plays a significant role [5], especially for high-strength materials [6].

It was shown earlier [7–10] that the description of the crystallographic orientations of the boundaries of the shear bands, which differ from the typical slip planes of ordinary dislocations, can be easily achieved using the concept of cristones. Cristons are generated by generalized Frank – Reed sources (GFRS), arising from strong (contact) interaction of dislocations with intersecting slip planes. When describing the orientation of the boundaries of shear bands using the cristones model, there is a simple connection with the fractional contribution of dislocations to the "composition" of the cristone. For example, for an face-centered cubic (fcc) lattice with only one family of slip planes $\{111\}$ and twelve slip systems, the simplest standard orientations of shear band boundaries are:

Email addresses for correspondence: mpk46@mail.ru

$$\{hh\ell\}, \qquad h/l=(n-m)/(n+m), \tag{1}$$

where n and m are integers, the moduli of which are equal to the number of dislocations of two contacting systems. Figure 1 shows a diagram of the formation of a dislocation “bundle” of two systems of dislocations along the line of intersection $\boldsymbol{\Lambda}\|\langle 1\text{-}10\rangle$ of a pair of slip planes. This "bundle" plays the role of the GFRS segment, characterized by the superposition Burgers vector $\mathbf{b}$:

$$\mathbf{b}\|n\mathbf{b}_1+m\mathbf{b}_2. \tag{2}$$

A slight simplification was made in the calculations. It is assumed that the vectors $\mathbf{b}_1$ and $\mathbf{b}_2$ have a purely edge orientation with respect to the working segment of the GFRS. It is clear that the curvature of the GFRS segment turns the Lomer - Cottrell type barrier into a source of dislocations sliding along the planes (hhl) to which $\mathbf{b}$ it belongs.

In the case of a bcc lattice, three families of planes can be active in the slip of dislocations: $\{110\}$, $\{112\}$ and $\{123\}$. The orientations $\{hhl\}$ of the boundaries of the shear bands are also inherent in alloys with a bcc lattice. If the configuration of the cristone core corresponds to pure shear deformation (see [8, 9]), then in the shear region there will also be a change in the orientation of the lattice. Thus, the cristone concept makes it possible to understand how the transition from the level of translational easy slip of individual dislocations to the mesoscopic level of the formation of shear bands with a changed orientation of the lattice occurs. Consequently, it is possible to use the crystallographic information on the evolution of shear bands to supplement the understanding of the mechanism of the formation of CLB. Further, for this purpose, the results of work [11] are analyzed, in which the formation of CPL was observed in polycrystalline samples with a bcc lattice, which have a pronounced texture after rolling.

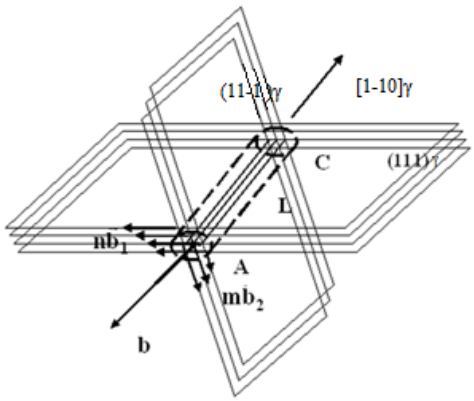

Fig 1. Formation of the working segment of the GFRS.

2. Experimental data

Fine-grained steel 08G2B (0.08 C, 1.87 Mn, 0.043 (Nb + Ti), 0.49 Cu) with a grain diameter of $d\approx 5$ μm was considered in [11]. Samples for subsequent stretching were cut so that the direction of stretching coincided with the direction of rolling, as shown in Figure 2. The digital image correlation method made it possible to measure elongation deformation ε_{yy} and shear deformation ε_{xy}. It was found that the formation of PCL is associated with the action of a stress mesoconcentrator, in the region of localization of which the component ε_{yy} reaches its maximum, while the component ε_{xy} is minimal. In contrast, the component ε_{xy} becomes maximum at the edges of the shear band. The formation of preferred orientations of crystals in local microvolumes, that is, the establishment of texture, was carried out by the method of diffraction of backscattered electrons (Electron Back-scattering Diffraction — EBSD). Figure 3 shows the intensity

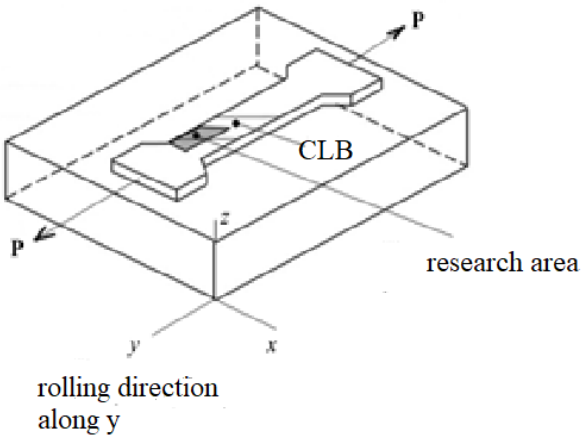

Fig 2. Tensile sample cutting scheme.

distribution of the four main types of texture components in different regions of the sample. The specification of the types of components is carried out by indicating the planes and directions of shear in the planes given in the orthogonal basis associated with the edges of the unit cell of the bcc lattice:

$$\text{Type I} — \{112\}\langle\text{-}110\rangle,\ \{113\}\langle\text{-}110\rangle,\ \{112\}\langle\text{-}311\rangle; \tag{3}$$

$$\text{Type II} — \{332\}\langle 02\text{-}3\rangle,\ \{332\}\langle 1\text{-}33\rangle,\ \{113\}\langle 3\text{-}61\rangle,\ \{112\}\langle 3\text{-}51\rangle; \tag{4}$$

$$\text{Type III} — \text{along plain } \{111\}; \tag{5}$$

$$\text{Тип IV} — \{001\}\langle 110\rangle. \tag{6}$$

Obviously, all the planes included in (3) - (6) are of the type, however, in contrast to the fcc lattice with a single family of octahedral slip planes, in the bcc lattice, cristone shear carriers are generated by a GFRS with $\mathbf{\Lambda}$ orientations of the working segments, in the general case, not collinear $\langle 1\text{-}10\rangle$ -directions. Note also that, after rolling, the texture is dominated by type I and type II components, while approaching the center of the CLB is characterized by an increase and predominance of type IV components.

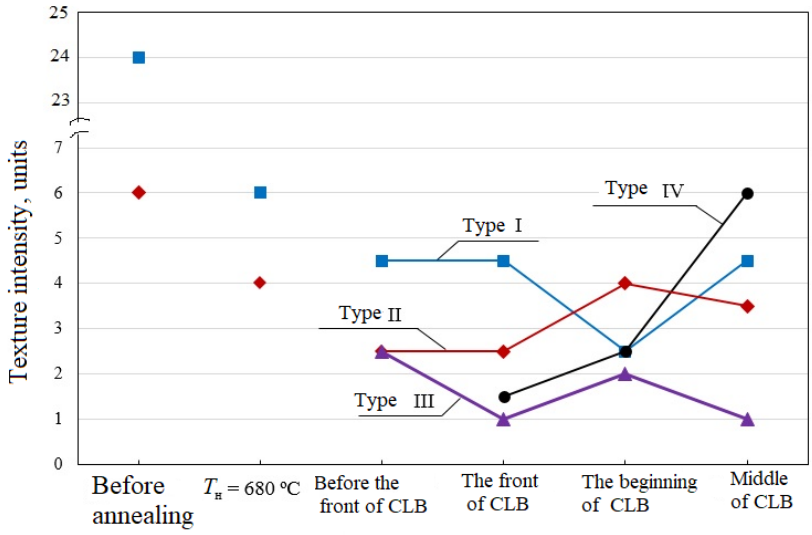

Fig . 3. Density of textural components in different parts of the CLB.

3. Comparison of the carriers of the shift of cristones with the observed components of the texture

Recall that the appearance of a rolling texture corresponds to the separation of some preferred directions from the initial set of chaotic orientations of crystal lattices of polycrystals (grains) with an indication of the planes that make up the smallest angles with the rolling surface after deformation. As you know, during rolling, the greatest deformation is compression, leading to a turn of the sliding planes in the direction of decreasing the angle between the sliding plane and the rolling plane (this turn is also supported by tension orthogonal to compression). It is obvious that shear processes with Burgers vectors exceeding Burgers vectors of single dislocations will lead to a higher strain rate. Therefore, it is natural to compare the observed texture components with cristone shear carriers characterized by superposition Burgers vectors $\mathbf{b}$. It should be borne in mind that to determine the orientation of the normal to the slip plane, it suffices to find the vector product $\mathbf{b}$ and $\mathbf{\Lambda}$

$$\mathbf{N} \| [\mathbf{b}, \mathbf{\Lambda}]. \tag{7}$$

From (7) it follows that the $\mathbf{N}$ orientation depends only on the edge (with respect to $\mathbf{\Lambda}$) component of the vector $\mathbf{b}$. Obviously, adding to the superposition vector a vector $\mathbf{b}$ of arbitrary magnitude, collinear to m, does not affect the fulfillment of condition (7), since the vector a is orthogonal to any direction. Obviously, if we add to the superposition vector $\mathbf{b}$ an arbitrary in magnitude vector $\mathbf{b}_{\|}$, collinear $\mathbf{\Lambda}$, then condition (7) will be satisfied, since the vector $\mathbf{b}_{\|}$ is orthogonal to any direction $[hhl]$. This means that when determining the vector $\mathbf{b}$ belonging to the (hhl) plane, an additive ambiguity arises:

$$\mathbf{b} \to \mathbf{b}' = \mathbf{b} + \mathbf{b}_{\|}. \tag{8}$$

Let us briefly dwell on the consequences arising from the proposed simplest model of the shift carrier. We recall that when a shift along a plane with a normal $\mathbf{N}$ in the direction $\mathbf{b}$ occurs, a material rotation around the axis $\boldsymbol{l}$ is realized:

$$\boldsymbol{l} \| [\mathbf{b}, \mathbf{N}], \tag{9}$$

where the symbol [,] means the vector multiplication operation. It is clear that for a purely edge orientation of the vector $\mathbf{b}$ relative to the line [1-10], the shift along the (hhl) plane will be accompanied by a material rotation around the axis $\boldsymbol{l} \| [1\text{-}10]$, that is, around the dislocation line.

Since the initial orientations $\boldsymbol{\Lambda}$ are given by the intersection lines of the initial slip planes, that is, the vector products of the normals of the intersecting planes, there is an extremely simple algorithm that allows one to compare the composition of the chrystons with the observed texture components, which show the relative contributions of the contact interacting dislocations to the resulting Burgers vector.

3.1. "Composition" of chrystones for texture components $\{112\}\langle\text{-}110\rangle$, $\{112\}\langle\text{-}311\rangle$, $\{112\}\langle 3\text{-}51\rangle$, related to slip systems on $\{110\}$ planes

Let us illustrate the definition of the “composition” of cristones for several cases, taking into account that the initial Burgers vectors in the bcc lattice correspond to half of the spatial diagonals of the unit cell, that is $\mathbf{b}_i = \langle 111 \rangle a/2$, where a is the lattice parameter. For further analysis, the value of a is insignificant and will be taken equal to 1. The factor 2 is not important either, so it can also be omitted as a common factor for all vectors. We define the resulting Burgers vector, as in (2), but with vectors $\mathbf{b}_i \| \langle 111 \rangle$. Let us consider the first variant $\{112\}\langle\text{-}110\rangle$ of the texture. We start with $\{110\}$ slip systems (SS) with the most dense packing of planes for a bcc lattice. Obviously, a pair of planes (101) and (011) corresponds to $\boldsymbol{\Lambda} \| [11\text{-}1]$, and a (112) slip plane is realized with the relation $n/m = 1/1$ in (2) for vectors $\mathbf{b}_1 \| [-111]$ and $\mathbf{b}_2 \| [\text{-}11\text{-}1]$. The texture $\{112\}\langle\text{-}311\rangle$, for example, $(112)[\text{-}311]$, results from the addition to the preceding vector $n(\mathbf{b}_1 + \mathbf{b}_2)$ of a vector $\mathbf{b}_3 \| n[\text{-}1\text{-}11]$ that is a multiple of the Burgers vector of a single dislocation from the SS (112), a screw orientation with respect to $\boldsymbol{\Lambda}$; in case $\{112\}\langle 3\text{-}51\rangle$, for example $(112)[\text{-}5\text{-}13]$, should be added to $3n[\text{-}1\text{-}11]$.

Thus, the textures $\{112\}\langle\text{-}311\rangle$ and $\{112\}\langle 3\text{-}51\rangle$ are associated not only with SS $\{110\}$, generating cristones and defining the shear plane, but also with large " screw" contributions from conventional for bcc lattices of dislocations belonging to the $\{112\}$ SS.

3.2. "Composition" of chrystones for texture components $\{112\}\langle\text{-}110\rangle$, $\{112\}\langle\text{-}311\rangle$, $\{112\}\langle 3\text{-}51\rangle$, related to slip systems on $\{123\}$ planes

There is also an additional cristone channel for the implementation of texture components $\{112\}\langle\text{-}110\rangle$, $\{112\}\langle\text{-}311\rangle$, $\{112\}\langle 3\text{-}51\rangle$ associated with the $\{123\}$ SS. Indeed, choosing, for example, a pair of planes (123) and $(12\text{-}3)$, we find $\boldsymbol{\Lambda} \| [\text{-}210]$. For $\mathbf{b}_1 \| [11\text{-}1]$ and $\mathbf{b}_2 \| [111]$ we get

$$\mathbf{b} \| [n+m,\ n+m,\ m-n], \qquad \mathbf{N} \| \left[m-n,\ 2(m-n),\ -3(n+m) \right]. \tag{10}$$

From (10) it follows that for $n = -2m$ the vector $\mathbf{N} \| [121]$, and $\mathbf{b} \| [11\text{-}3]$. It is clear that adding vectors $\mathbf{b}_\Lambda$, collinear $\boldsymbol{\Lambda} \| [2\text{-}10]$, to $\mathbf{b} \| [11\text{-}3]$, we can easily find additional observable shear directions:

$$\mathbf{b} + \mathbf{b}_\Lambda \| [11\text{-}3] + [2\text{-}10] = [30\text{-}3] \| [10\text{-}1], \qquad \mathbf{b} + 2\mathbf{b}_\Lambda \| [11\text{-}3] + 2[2\text{-}10] = [5\text{-}1\text{-}3]. \tag{11}$$

However, the formal procedure (11) now stands not only for the addition of the existing dislocations with vectors that are multiples of $\mathbf{b}_i \| \langle 111 \rangle$, but for the superposition Burgers vectors arising in the contact cristone- cristone interaction. This is easy to understand, taking into account that the Burgers vector $\mathbf{b}_\Lambda$ belongs to the (001) plane and, therefore, can be summed up with the cristone vector $\mathbf{b}$, when the section of the cristone loop of the cubic slip is included in the working segment of the GFRS, since the planes (121) and (001) intersect along $\Lambda \| [2\text{-}10]$.

3.3. Composition" of chrystones for texture components $\{001\}\langle 110\rangle$, related to slip systems on $\{110\}$ or $\{112\}$ planes

Cubic slip arises as a result of the contact interaction of dislocations capable of sliding in the $\{110\}$ or $\{112\}$ planes. Let us show it. For definiteness, we choose a pair of slip planes (110) and $(1\text{-}10)$. Then the line of intersection of the planes is $\Lambda \| [001]$. For $\mathbf{b}_1 \| [1\text{-}11]$ and $\mathbf{b}_2 \| [111]$ we have:

$$\mathbf{b} \| [n+m,\ m-n,\ n+m]. \qquad (12)$$

It follows from (12) that for $n = m$ cubic slip along the (010) plane is associated with the vector $\mathbf{b}_1 \| [101]$, and for $n = -m$ slip is possible along the (100) plane with the vector $\mathbf{b}_2 \| [010]$. Accordingly, for a pair of slip planes (112) and $(11\text{-}2)$ we find $\Lambda \| [1\text{-}10]$. For $\mathbf{b}_1 \| [11\text{-}1]$ and $\mathbf{b}_2 \| [111]$ we get:

$$\mathbf{b} \| [n+m,\ n+m,\ m-n]. \qquad (13)$$

From (13) it follows that for $n = m$, cubic sliding along the (001) plane is associated with the vector $\mathbf{b}_1 \| [110]$, and for $n = -m$, sliding is possible along the (110) plane with the vector $\mathbf{b}_2 \| [001]$.

3.4. Summary table of the "composition" of chrystones for the observed texture components

Proceeding in a similar way, it is easy to find the ratio of n and m for all the resulting texture components. For specific options, this is demonstrated in the summary Table.

Table. Determination of "compositions" of chrystones for texture components.

Types of observable texture components	Active sliping systems	Slip (shear) planes of cristones	Shear directions in the crystal model	Orientation of the rotate axis in the shear band	«Composition» n/m
Type I	$(101)[\text{-}111]$ $(1\text{-}10)[111]$	$(2\text{-}11)$	$[022] \| [011]$ $[022]+[11\text{-}1]=[131]$	$[11\text{-}1]$	1/1
	$(123)[11\text{-}1]$ $(12\text{-}3)[111]$	(121)	$[11\text{-}3]$	$[\text{-}210]$	2/-1
	$(110)[1\text{-}11]$ $(112)[11\text{-}1]$	$(\text{-}131)$	$[4\text{-}22]$ $[4\text{-}22]\text{-}2[1\text{-}10]=[101]$	$[1\text{-}10]$	3/1
Type II	$(101)[\text{-}111]$ $(1\text{-}10)[111]$	$(2\text{-}11)$	$[022]$ $[022]+3[11\text{-}1]=[35\text{-}1]$	$[11\text{-}1]$	1/1
	$(112)[11\text{-}1]$ $(11\text{-}2)[111]$	(332)	$[11\text{-}3]$ $[11\text{-}3]+[1\text{-}10]=[20\text{-}3]$ $[11\text{-}3]+2[1\text{-}10]=[3\text{-}1\text{-}3] \| [\text{-}313]$	$[1\text{-}10]$	2/-1

Type III	$(112)[11\text{-}1]$	(111)	$[22\text{-}4]$	$[1\text{-}10]$	3/-1
Type IV	$(11\text{-}2)[111]$	(001)	$[220]$		1/1

Note that in order to obtain a complete set of experimental shear directions, it is necessary to add components collinear to the directions of the GFRS segments to the initial criston Burgers vector.

For example, for the border of a strip with orientation n, the Burgers vector, which is compared with the cristone describing the first observed shear direction, contains an additional contribution - a component along the GFRS segment. Subsequent addition to the Burgers vector of a similar contribution gives the second tracked direction of the shift. For example, for the border of a band with orientation (332), the Burgers vector, which is compared with the cristone describing the first observed shear direction, contains an additional contribution - a $[1\text{-}10]$ component along the GFRS segment. Subsequent addition to the Burgers vector of a similar contribution gives the second tracked direction of the shift.

3.5. Generalizing comments

An analysis of the texture showed that all the initial systems of dislocation slip, typical of crystals with a bcc lattice, can participate in its formation, and they can lead to the appearance of GFRS and cristone shear carriers upon contact interaction. Taking into account the emergence of variants cristone of shear during the developing plastic deformation (including due to cristone-cristone interactions) removes, in the opinion of the authors of this work, the question of the non-Schmidov nature of sliding discussed in [12] using the example of an alloy with an fcc lattice. Preliminary texturing of the initial misoriented polycrystalline medium and its saturation with mesoconcentrators (similar to GFRS) are factors contributing to the manifestation of collective effects in ensembles of interacting defects. These effects include not only the appearance of hierarchical strip structures, including CLB, but also destruction processes [13]. Texturing favors ordering in the intercrystalline medium, the proportion of which increases with a decrease in the size of the polycrystals. The formation of CLB, as shown by the data [11], is associated with the action of a certain stress macroconcentrator, the size of which exceeds the grain size. It seems likely that such a concentrator will form in a sufficiently large group of contacting grains with a similar texture. This is connected with the process of interaction of the GFRSs present in the grains, including the processes of creeping cristone loops up to the synthesis of the macroconcentrator. An intergranular medium in the presence of texture and a sufficient number of vacancies can combine quasicrystalline (anisotropic) properties with those of a viscous liquid. Thus, the analysis of the texture within the framework of the cristone approach provides additional information for refining the physical concepts of the mechanisms of formation of CLB.

4. Conclusion

1. Cryston schemes for the implementation of deformation processes made it possible to interpret all the texture components traced during tension of an alloy with a fine-grained structure after preliminary rolling.
2. The enrichment of the CLB center with the $\{001\}\langle 110\rangle$ component corresponds to equal contributions from contact interacting dislocations and leads to the greatest deviation of the shear band boundaries from the orientation of the plane $\{112\}$. taken as a reference. This is consistent with the change in the orientations of the shear bands observed in [11] during the development of the CLB.
3. In the cristone scheme, the occurrence of the GFRS is a universal factor. In the presence of a polycrystalline structure, the GFRS size is limited by the grain size. It seems promising to develop a model for the formation of a macroconcentrator of stresses as a consequence of the interaction of GFRS in a group of contacting grains.
4. Known scenarios for the formation of CLBs, similar to nonequilibrium phase transitions in a system of defects, including the autowave description [3, 14], can apparently be refined and supplemented by taking into account (along with dislocations and disclinations) cristones.

The authors are grateful to A.N. Morozova for the experimental data presented in [11], as well as to the participants of the XXII Winter School on Continuum Mechanics (March 22-26, 2021, Perm) for valuable

comments when discussing the results. The work was carried out within the framework of the state assignment of the Ministry of Science and Higher Education of the Russian Federation No. 075-00243-20-01 of August 26, 2020 (topic FEUG-2020-0013 "Environmental aspects of rational nature management").

References

1. Vladimirov V.I., Romanov A.E. *Disklinatsii v kristallakh* [Disclinations in crystals]. Leningrad, Nauka, 1986. 224 p.
2. Panin V.E. (ed.) *Strukturnyye urovni plasticheskoy deformatsii i razrusheniya* [Structural levels of plastic deformation and destruction]. Novosibirsk, Nauka, 1990. 255 p.
3. Zuyev L.B., Danilov V.I., Barannikova S.A. *Fizika makrolokalizatsii plasticheskogo techeniya* [Physics of plastic flow macrolocalization]. Novosibirsk, Nauka, 2008. 328 p.
4. Gorbatenko V.V., Danilov V.I., Zuev L.B. Plastic flow instability: Chernov–Lüders bands and the Portevin-Le Chatelier effect. *Tech. Phys.*, 2017, vol. 62, pp. 395-400. https://doi.org/10.1134/S1063784217030082
5. Panin V.E., Panin A.V., Elsukova T.F., Popkova Yu.F. Fundamental role of crystal structure curvature in plasticity and strength of solids. *Phys. Mesomech.*, 2015, vol. 18, pp. 89-99. https://doi.org/10.1134/S1029959915020010
6. Tyumentsev A.N., Korotayev A.D., Ditenberg I.A., Pinzhin Yu.P., Chernov V.M. *Zakonomernosti plasticheskoy deformatsii v vysokoprochnykh i nanokristallicheskikh materialakh* [Regularities of plastic deformation in high-strength and nanocrystalline materials]. Novosibirsk, Nauka, 2018. 256 p. http://dx.doi.org/10.15372/Deformation2018TAN
7. Kashchenko M.P., Letuchev V.V., Yablonskaya T.N., Teplyakova L.A. A model of the formation of macroshear bands and strain-induced martensite with (hhl) boundaries. *Phys. Metals Metallogr.*, 1996, vol. 82, pp. 329-336.
8. Kashchenko M.P., Chashchina V.G., Semenovih A.G. Cryston model of shear band formation in cubic crystals with crystallographic orientation of random-type boundaries. *Fiz. mezomekh. – Phys. mesomech.*, 2003, vol. 6, no. 1, pp. 95-122.
9. Kashchenko M.P., Chashchina V.G., Semenovykh A.G. Cryston model of formation of strain-induced α'-martensite in fe-based alloys. *Fiz. mezomekh. – Phys. mesomech.*, 2003, vol. 6, no. 3, pp. 37-56.
10. Kashchenko M.P., Chashchina V.G. Crystons: basic ideas and applications. *Lett. Mater.*, 2015, vol. 5, pp. 82-89. https://doi.org/10.22226/2410-3535-2015-1-82-89
11. Farber V.M., Morozova A.N., Khotinov V.A., Karabanalov M.S., Schapov G.V. Plastic flow in a Chernov–Luders band in ultrafine-grained 08G2B steel. *Phys. Mesomech.*, 2020, vol. 23, pp. 340-346. https://doi.org/10.1134/S1029959920040086
12. Ranjan D., Narayanan S., Kadau K., Patra A. Crystal plasticity modeling of non-Schmid yield behavior: from Ni_3Al single crystals to Ni-based superalloys. *Modelling Simul. Mater. Sci. Eng.*, 2021, vol. 29, 055005. https://doi.org/10.1088/1361-651X/abd621
13. Naimark O., Bayandin Yu., Uvarov S., Bannikova I., Saveleva N. Critical dynamics of damage-failure transition in wide range of load intensity. *Acta Mech.*, 2021, vol. 232, pp. 1943-1959. https://doi.org/10.1007/s00707-020-02922-1
14. Zuyev L.B., Barannikova S.A., Lunev A.G. *Ot makro k mikro. Masshtaby plasticheskoy deformatsii* [From macro to micro. The scale of plastic deformation]. Novosibirsk, Nauka, 2018. 130 p.

The authors declare no conflict of interests.
The paper was received on 15.04.2021.
The paper was accepted for publication on 20.05.2021.